PETROLOGY, GEOCHEMISTRY AND DEPOSITIONAL ENVIRONMENT OF THE KHABOUR FORMATION IN ORA AND KHABOUR LOCALITIES, NORTHERN IRAQ

Khaldoun S. Al-Bassam*

Received: 24/ 11/ 2009, Accepted: 2/ 6/ 2010
Key words: Khabour Formation, Depositional environment, Iraq

ABSTRACT

The Khabour Formation, the oldest exposed rock unit in Iraq (Ordovician), was sampled in two exposed sections at Ora and Khabour localities. It is comprised of about 800 m thick sandstone-shale cyclic alternations. Petrographic study showed that quartz arenite and phyllarenite are the main textural varieties of the sandstone with mica and silt-size quartz dominating the shale. The sandstones are texturally mature and mineralogically mature to submature. The mineralogy includes: quartz (dominant), muscovite, illite, glauconite, chlorite/serpentine (mixed layer), francolite (conodont) and heavy minerals (opaques and ZTR). Silica cementation is the main diagenetic process, resulted from pressure solution of silica and lead to an interlocking quartz mosaic texture. Alteration is of minor intensity.

The chemical composition is characterized by high SiO_2/Al_2O_3 and K_2O/Na_2O ratios. The geochemical associations are controlled by the mineralogy and three groups were recognized by factor analysis, namely the sheet alumino-silicates, phosphate and heavy minerals (ZTR). All of which are diluents to the major mineral constituent: quartz.

Mineralogical analysis of the studied samples suggests recycled granitic plutonic rocks and more proximal low-grade metamorphic rocks as source of the clastics. The whole sequence of the Khabour Formation seems to have deposited in marine environment extending from shallow intertidal to deep outer shelf, under variable conditions of sea-level fluctuation, subsidence rate, and detritus supply. The whole sequence may have resulted from deposition from turbidity currents; the proximal part is rich in coarse clastics and the distal part is rich in micaceous shale. Complete Bouma sequence was not recognized, but the sedimentary facies of the Khabour Formation may be considered as an example of a passive plate margin turbidities.

صخارية وجيوكيميائية والبيئة الترسيبية لتكوين الخابور في مناطق أورا والخابور، شمال العراق

خلدون صبحي البصام

المستخلص

يعتبر تكوين الخابور أقدم التكوينات الجيولوجية المتكشفة في العراق ويقدر عمره بالاوردوفيزي وتقع مكاشفه في أقصى شمال العراق في منطقتي أورا والخابور وقد تم التعرف على التكوين أو مكافآته الصخرية والعمرية مع بعض الاختلافات السحنية الطفيفة تحت السطح في مقاطع آبار الخليصية في منطقة الجزيرة وعكاس في الصحراء الغربية، فضلاً عن عدد من الدول المجاورة مثل الأردن وسوريا والسعودية وتركيا.

لم يحظ هذا التكوين بدراسات حديثة في مقاطعه المتكشفة في العراق وما أنجز في هذا المجال يعود إلى حوالي نصف قرن من الزمن.

لأغراض البحث الحالي، جرت نمذجة لتكوين الخابور في مقطعين متكشفين في منطقتي أورا والخابور، حيث يتألف التكوين من حوالي 800 متر من تتابع دوري من الحجر الرملي والسجيل. يتدرج الحجر الرملي نحو حجم الغرين باتجاه الأعلى لينتهي بطبقات السجيل تدريجياً غير أن حد الاتصال مع الدورة الأعلى يكون حاداً ومتميزاً بوجود المايكا والكثير من التراكيب الرسوبية مثل الحفريات وآثار الكروزيانا.

* Chief Researcher, State Co. of Geological Survey and Mining, P.O. Box 986 Alwiya, Baghdad.
e-mail: khaldoon47@yahoo.com

بلغ عدد العينات في هذه الدراسة 26 عينة جرى فحصها مجهرياً من خلال الشرائح الرقيقة فضلاً عن فصل وتشخيص المعادن الثقيلة. كما تم تحليل العينات كيميائياً للأكاسيد:
SiO_2, TiO_2, Fe_2O_3, Al_2O_3, CaO, MgO, K_2O, Na_2O, P_2O_5, ZrO_2 وتحليل عينات مختارة لعنصر الفلور.
اعتمدت تقنية حيود الأشعة السينية لدراسة المعادن الصفائحية (المايكا والأطيان) والمعادن الأخرى المكونة للسجيل وبعض عينات الحجر الرملي.

أظهرت الدراسة الصخرية المجهرية ان الحجر الرملي من نوعين: الكوارتز أرينايت والفيلارينايت في حين يتكون السجيل من المايكا والكوارتز الغريني وبينت ان الحجر الرملي دقيق التحبب وجيد الفرز، يوجد احياناً بدون حشوة وأحياناً أخرى مع حشوة من المايكا بكافة معادنها. كما بينت الدراسة نضوج الصخور الرملية من ناحية النسيج المجهري وناضجة إلى غير ناضجة من الناحية المعدنية.

يتكون التركيب المعدني من الكوارتز (المعدن السائد)، المسكوفايت، الإلايت، الغلوكونايت، الكلورايت (متداخل الطبقات مع السربنتين)، الفرنكولايت (كونودونت) والمعادن الثقيلة (المعتمة والزركون والتورمالين والروتايل). العملية التحويرية الرئيسية هي الإلتحام بالسيليكا الناتجة عن إذابة السيليكا تحت الضغط وإعادة ترسيبها لتعطي مظهراً موزائيكياً متداخلاً لحبيبات الكوارتز. التغيرات التحويرية ظهرت قليلة نسبياً وتميزت بتغير محدود للفلدسبار (بلاجيوكليز) إلى المايكا وتحول الكلورايت الى كلورايت/ سربنتين. إن وجود معدن الفرنكولايت (موقعي النشأة) في هذا التكوين يأشر أقدم ظهور للفوسفات الرسوبي البحري في التكوينات الجيولوجية العراقية ويمكن أن يرتبط ترسيبه ببداية انطلاق دورة من دورات الطغيان البحري المتعاقبة التي سادت الحوض الرسوبي أثناء ترسيب تكوين الخابور.

يتميز التركيب الكيميائي بنسب عالية من السيليكا إلى الألومينا ومن البوتاسيوم الى الصوديوم ويتحكم التركيب المعدني بالارتباطات الجيوكيميائية حيث تم تمييز ثلاثة مجاميع على ضوء التحليل العاملي: الأول يتحكم بالمعادن الصفائحية الألومينية السيليكية والثاني يتحكم بالمكونات الفوسفاتية والثالث بالمعادن الثقيلة وجميع هذه الفصائل المعدنية تعتبر مخففات للمعدن الرئيسي السائد وهو الكوارتز ولها علاقة سالبة معه.

يشير التحليل المعدني لعينات الدراسة إن صخور المصدر من نوعين الأول صخور غرانيتية بلوتونية معادة الترسيب والثاني مصدر أقرب من الصخور المتحولة ذات الرتبة الواطئة ويبدو أن التتابع بكامله قد ترسب في بيئة بحرية تمتد من المناطق الضحلة المتأثرة بالمد البحري إلى المناطق العميقة من الرف الخارجي وتحت ظروف متباينة من تذبذب في مستوى سطح البحر ونسبة الهبوط في الحوض الرسوبي والتغذية بالفتاتيات من المصدر. يمكن تفسير الترسيب الدوري للفتاتيات (رمال، غرين، أطيان) إلى تداخل عدة عوامل جيولوجية مؤثرة مثل تذبذب في مستوى سطح البحر لأسباب بنيوية أو مناخية وكمية الفتاتيات الواردة إلى الحوض الرسوبي من مناطق المصدر والترسيب الدوري النموذجي للطبقات المتدرجة لرواسب الكدرة (تتابع بوما). يتميز الجزء الأعلى من التتابع بسيادة سحنة السجيل التي تشير إلى طغيان بحري واضح. إن كامل التتابع قد يكون قد ترسب من تيارات كدرة، الجزء القريب منها غني بالفتاتيات الخشنة والجزء البعيد غني بالسجيل المحمل بالمايكا وعلى الرغم من عدم ملاحظة وجود تتابع بوما متكامل غير ان تكوين الخابور يمكن اعتباره نموذجاً لرواسب الكدرة (التربيدايت) التي تتكون في حافات الصفائح الخاملة. ويسند ذلك المعطيات الجيوكيميائية التي تشير إلى النسب العالية من السيليكا إلى الالومينا والبوتاسيوم الى الصوديوم والنسيج الصخري العام لصخور الدراسة والترسيب الدوري للتابع فضلاً عن اتفاق الوضع الجغرافي القديم للمنطقة مع هذا الإستنتاج.

INTRODUCTION

The Khabour Formation, about 800 m exposed thickness of sandstone-shale association in the type section, is the oldest rock unit exposed in Iraq dated as Ordovician. It was first described by Wetzel (1950) in the area North of Zakho, in the valley of the Khabour River, where the formation got its name and where the type section is located. Later it was encountered in subsurface sections in Khleisia-1 well in the Al-Jazira area (Gaddo and Parker, 1959 and Ditmar *et al*., 1971) and in Akkass-1 well in the Western Desert (Habba *et al*., 1994 and Aqrawi, 1998).

The Khabour Formation was encountered and compared, on the basis of age and lithology, to several rock units in SE Turkey, E Jordan, Syria and Saudi Arabia (Buday, 1980; Aqrawi, 1998; Sharland *et al.,* 2001 and Jassim and Goff, 2006). Due to the remoteness and difficult accessibility of the area, the exposed sections of the Khabour Formation in Iraq were not studied in detail. All the previous work dealt with field examination of outcrops, except where paleontological studies, for age determination, were carried out in the early works.

The purpose of this work is to study the petrology, mineralogy and chemical composition of the Khabour Formation in two sections exposed in Ora and Khabour localities, N Iraq and to synthesis the results to have an updated view on the depositional environment.

PREVIOUS WORK

- Wetzel (1950) was the first who mapped and described the Khabour Formation in N Iraq and suggested the age Cambro – Ordovician for the exposed parts. He presented a detailed description of the lithology of the formation and its contacts.
- Gaddo and Parker (1959) studied the formation in subsurface section of Khleisia-1 oil well in Al-Jazira area and compared the encountered sequence with the Khabour Formation exposed in north Iraq. They reconsidered the age and established Middle to Late Ordovician (Llandeilo) age for the formation.
- Seilacher (1963) restudied the formation in N Iraq exposures and confirmed the age as Ordovician. He suggested deeper marine environment for the upper parts where he recognized a turbidite-affected deeper facies.
- Al-Hadithi (1972) presented the mapping results of GEOSURV team in the area. The information included field description of the exposed sections in N Iraq and considered the sequence flysh-like sediments. The results suggested Ordovician (Llandeilo?) for the upper parts.
- Isa'ac (1975) continued GEOSURV work in N Iraq and described the Khabour Formation in exposed sections. The results showed a thin hematitic – miacaceous quartzite horizon at the top of the formation and confirmed the Ordovician (Llandeilo) age.
- Buday (1980) critically studied the available information on the Khabour Formation and compared it with equivalent rock units in neighboring countries.
- Habba *et al.* (1994) studied the Paleozoic sequences in subsurface sections drilled in the Western Desert and identified age-and lithological-equivalent to the Khabour Formation in Akkas oil well-1.
- Aqrawi (1998) studied the Paleozoic stratigraphy in Western and Southwestern deserts of Iraq including the Khabour Formation in Akkas oil well-1.
- Sharland *et al.* (2001) studied the sequence stratigraphy of the Arabian Plate and came to mention the Khabour Formation in several occasions and considered it to mark the last sedimentary stage of a transgressive – regressive cycle.
- Jassim and Goff (2006) in a comprehensive compilation of the geology of Iraq, they considered the Khabour Formation as the Mid-Late Ordovician sequence of the Late Cambrian – Early Ashgill Megasequence.
- Tamar-Agha (2009) published the only detailed petrographic and mineralogical study of the Risha Sandstone Member (Late Ordovician) in subsurface sections of the Risha Gas Field of Jordan, which is considered equivalent to the Khabour Formation in Iraq. He studied the influence of cementation on reservoir quality and classified the rocks as sub arkoses and quartz arenites and texturally mature to supermature. He provided a generalized model of digenetic paragenesis with special emphasis on cementation.

GEOLOGICAL SETTING

The Khabour Formation is about 800 m thick in exposed section of the type area. It is unconformably overlain by the Pirispiki Formation (Wetzel, 1950). The unconformity is believed erosional and marked in Iraq by the Chalki Volcanics (Sharland *et al.*, 2001).

The lithology, as described by Wetzel (1950), consists of alternation of thin-bedded, fine grained sandstones, quartzites and silty micaceous shales, olive green to brown in color. The quartzites are generally cross bedded and the bedding planes are well surfaced with smooth films of greenish micaceous shales. The quartzite beds are occasionally truncated by overlying beds. The sedimentary structures observed in the Khabour Formation at the exposed sections include laminations, ripple marks, load casts, slump structures, trace fossils, cross bedding, fucoid markings, infilled trails, burrows and pitted surfaces (Wetzel, 1950; Al-Hadithi, 1972 and Isa'ac, 1975). Based on *Cruziana* sp. tracks throughout the section, the age was given by Wetzel (1950) as Cambro – Ordovician. However, in later works, the age was determined as Middle to Late Ordovician (Llandeilo) (Seilacher, 1963). More recent works (Sharland *et al*., 2001 and Jassim and Goff, 2006) accepted the age of the Khabour Formation as Caradoc to Ashgill.

The Khabour formation is believed to have deposited in a tide- and storm-dominated shallow marine intertidal environment of mud- and silt-flats with occasional emergence (Wetzel, 1950).

Deeper environment was suggested for the upper parts of the formation in the type section, where turbidite-affected deeper facies were recognized by Seilacher (1963). According to Jassim and Goff (2006), the formation, in outcrop sections, passes from littoral facies in the "Ora anticline" into a deeper marine turbidite facies in "Kaista anticline" (Khabour area).

Based on the observation made by the present author the Khabour Formation consists of cyclic alternations of fining upward sequences of sandstone-siltstone and silty micaceous shale with well-defined upper surfaces of individual cycles. Thicker bedding of sandstone dominates the lower part which becomes thinner and grades into silty shale in the upper part. (Figs.1 and 2).

In the lower part of the formation, thick quartzite beds alternates with thin silty shale horizons. The upper contact of the shale horizons is sharply terminated and bioturbated. Micaceous minerals form smooth surfaces with metallic luster marking the upper contact of each cycle. The quartzite is generally fine grained, often laminated and occasionally bioturbated. The silty shale is ferruginous, slope-forming, ranging in thickness from few centimeters (in the lower part) to few meters (in the upper part). Nodules of Fe-oxyhydroxides are occasionally found in the silty shale. The sedimentary structures observed in the present study are cross bedding (Fig.3), infilled trails and borings (Fig.4), burrowings (Fig.5), slump structures (Fig.6), dark laminations (Fig.7) and *Cruziana* burrowings and imprints (Fig.8).

Sharland *et al.* (2001) studied the sequence stratigraphy of Arabia and they considered the Khabour Formation (and other equivalent rock units in the region) to represent the concluding stage of the 75 m.y. long tectonostratigraphic megasequence (AP2). The lithological character of alternating shale-sand was suggested by these authors to indicate significant changes in relative sea-level, accommodation space and sediment supply. They considered the Khabour Formation to mark the last sedimentary stage of a transgressive-regressive cycle. The top of the (AP2) megasequence is marked by a strongly erosional unconformity, evident by the Chalki Volcanics in Iraq, and marking the onset of a major back-arc rifting and basaltic volcanism at the northern end of Arabia associated with the beginning of a SW-directed subduction beneath the plate (Beydoun, 1991 and Sharland *et al*., 2001).

SAMPLING AND METHODS

▪ Sampling

Two major sections were sampled, namely Khabour and Ora Sections (Fig.9). The former included four sampling stations as follows from older to younger: Station K/1: one sample, Station K/2: five samples, Station K/3: three samples and Station K/4: three samples. The latter included three stations, they are from older to younger: Station O/3: four samples, Station O/2: six samples and Station O/1: four samples. The total number of samples collected is 26 samples.

The samples consisted of sandstones and shale. The former were studied in thin sections using GEOSURV standard Work Procedures, Part 18 (Tamar-Agha and Mahdi, 1992) as well as textbooks on sandstone petrology (Folk, 1974 and Pettijohn *et al*., 1986). The shale samples, together with some selected sandstone samples, were examined by X-ray diffraction, using Shimadzu XRD 7000 instrument and following GEOSURV standard Work Procedures, Part 21 (Al-Janabi *et al*., 1992), (Figs.10 and 11).

All samples were chemically analyzed in GEOSURV Central Laboratories using GEOSURV standard Work Procedures, Part 21 (Al-Janabi *et al.*, 1992). The oxides and elements analyzed are: SiO_2, TiO_2, Fe_2O_3, Al_2O_3, CaO, MgO, K_2O, Na_2O, P_2O_5 and ZrO_2. Most of the oxides were analyzed by X-ray fluorescence spectrometry using Shimadzu XRF 1800 instrument. Selected samples were analyzed for F using ion selective electrodes. Moreover, heavy minerals were examined in selected sandstone samples using heavy liquid separation as in GEOSURV standard Work Procedures, Part 18 (Tamar-Agha and Mahdi, 1992). Statistical treatment of chemical analysis data included correlation coefficients and factor analysis using Principle Component Analysis Method.

Fig.1: Sampling station No.4 in the Khabour locality.
Medium bedded, graded sandstone interbedded with very thin silty shale horizons

Fig.2: Sampling station No.5 in the Khabour locality.
Thin and medium bedded fine grained sandstone
interbedded with silty shale with *Cruziana* trails

PETROGRAPHY AND MINERALOGY

▪ Framework Grains

– **Quartz:** Is the dominant mineral among the detrital constituents of the sandstone. It forms more than 95% of the detrital grains in the lower parts of the sampled sections and mostly at the base of the cycles where the sandstone may be classified as quartz arenite (Folk, 1974 and Pettijohn *et al*., 1986). The quartz is fine grained, moderately well sorted, subangular to subrounded and monocrystalline (Figs.12, 13 and 14). Interlocking compound quartz grains with sinuous outlines are common, (Fig.13) especially at the base of the cycles, where it is matrix-free and quartz may form more than 90% of the sandstone constituents. The quartz grains approach silt-size in the upper parts of the cycle and its content is reduced to less than 50% of the constituents with an open framework texture, filled with sheet silicate matrix (Fig.14).

– **Feldspars:** Are present in very minor proportion. They are composed mostly of plagioclase, showing polysynthetic twining (Fig.15), and to a lesser extent microcline (Fig.16). They are fine to very fine grained, generally fresh, but occasional diagenetic alteration of plagioclase to smectite (?) can be noticed (Fig.17). It usually shows a presence in XRD patterns (as albite) (Figs.10 and 11).

– **Muscovite:** Is a dominant detrital framework constituent in the Khabour Formation, present as elongated flakes deformed and bended, occasionally buckled (Fig.14), and forms the major detrital constituent at the top of the cycles commonly as bed-surface lining. In XRD patterns, the 001 reflection of muscovite is usually accompanied by major reflections of other mica minerals (such as illite and glauconite) (Fig.11b), but occasionally it is sharp and indicates high crystallinity (Fig.11a).

– **Francolite:** Is a rare framework constituent in the studied samples. It was recognized by XRD in one sample only (Fig.10c) as conodont (?) remains (Fig.19), bioclasts (Fig.20) and cortoids (Fig.21). The francolite grains are of larger size than the quartz, and appear to have formed authigenically. The skeletal phosphatic elements may be related to conodonts remains, which thrived in the Ordovician (Muller, 1978 and Cooper, 1981). However, this assumption requires detailed paleontological work to be verified.

– **Heavy minerals:** They are present in the studied samples in considerable amounts; ranging from (7 – 19) % of the (63 – 250) μm size fractions. The opaques make most of the heavies (27 – 74 %). Zircon, tourmaline and rutile (ZTR) form the major transparent heavies (18 – 70 %). Occasionally, chlorite is present in significant amounts reaching up to 30% of the transparent heavies. (Sample 0/3/4) (Table 1 and Fig.22). Anatase and ulvospinel (Fe_2TiO_4) are among the opaque heavy minerals and were identified in the XRD scans of the heavy fraction in considerable concentrations (Fig.29).

▪ Matrix

Crushed muscovite and illite are the main matrix minerals in the Khabour sandstone. Matrix constituents increase upward in each cycle and appear as crushed fragments filling space between quartz grains. Basal parts of the cycles contain less matrix constituents. Interstratified chlorite/serpentine rarely forms some of the matrix and/or cement's constituents, present as elongate fibers, isolated or buckled (Fig.23) and confirmed by X-ray diffraction (Fig.11) (Reynolds *et al*., 1999). It was recognized in a few samples only with an outstanding presence in sample (0/3/1), forming shiny surface lining of sandstone beds.

Fig.3

Fig.4

Fig.5

Fig.6

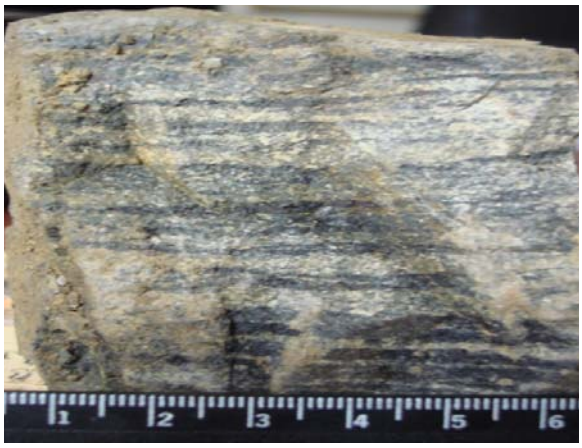

Fig.7

Fig.8

Fig.3: Cross lamination in sandstone (Ora)
Fig.4: Infilled trails and borings parallel to bedding (Ora)
Fig.5: Vertical burrowing in sandstone (Ora)
Fig.6: Slump structure (Ora)
Fig.7: Heavy minerals laminations in sandstone (Ora)
Fig.8: *Cruziana* imprints in shale (Ora)

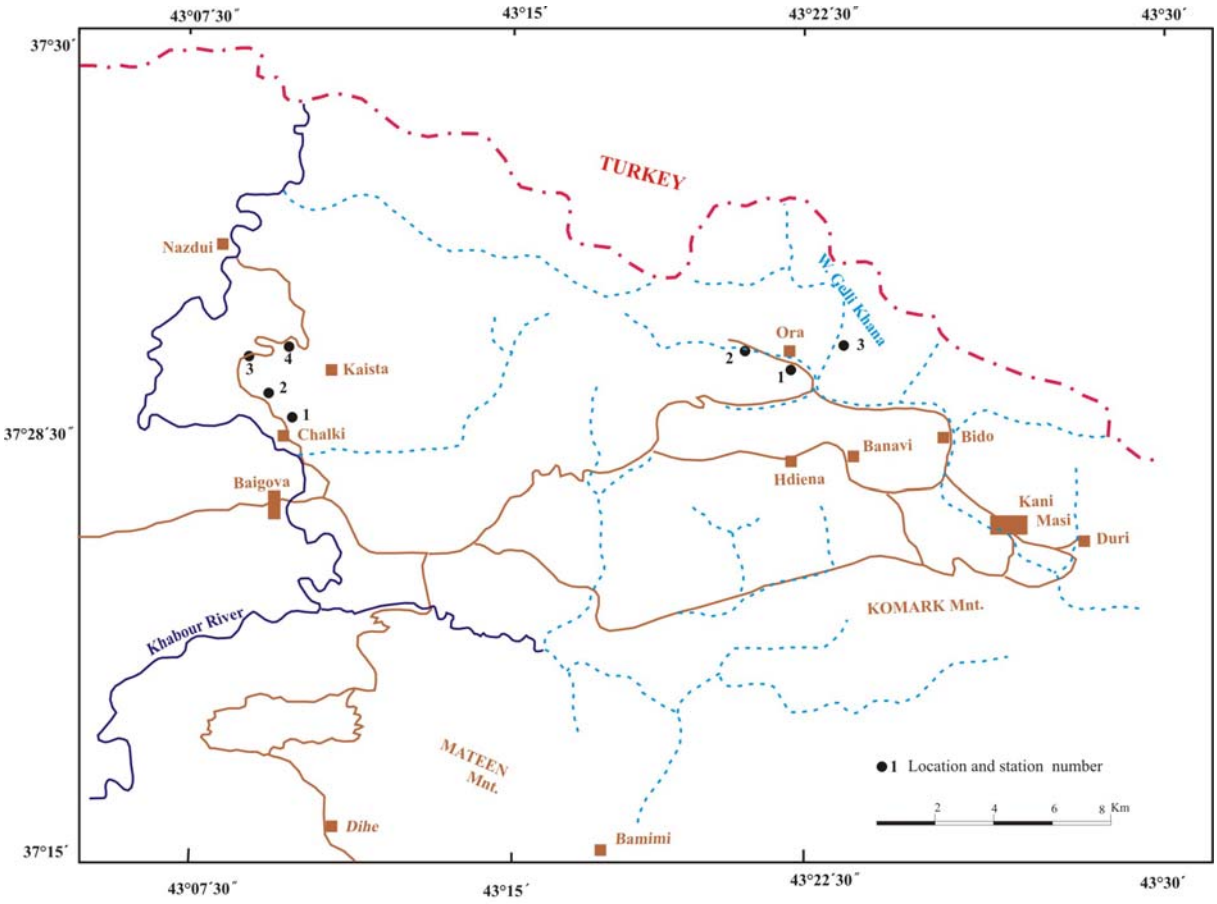

Fig.9: Location map of the studied samples

- **Cement**

Quartz overgrowths in the quartz arenites are the main cementing material in the Khabour sandstones. The quartz cement in this case produces a mosaic of interlocking grains (Fig.13). The original outlines of the detrital quartz grains are diffused and the "secondary" quartz cement resulted in interlocking and suturing of grain boundaries and producing a "false" angular outer shape. The dust line usually appears in such sandstones but it was difficult to see in the studied samples, which may indicate successive and intense pressure solution and silica precipitation after deep burial. Silica, as coarse crystals, cement fracture-openings in the sandstone (Fig.24). Clay minerals, including smectite, and illite are occasionally observed filling intergranular space and identified by XRD (Fig.10). Authigenic interstratified chlorite/ serpentine was occasionally observed in thin sections around some quartz grains (Fig.25) or associated with stylolites (Fig.26). Authigenic chlorites of this type are common in sandstones and may form within 1.8 Km of burial (Grigsby, 2001). Glauconite is a common authigenic constituent, present as rounded to subrounded grains, larger in size than the quartz, green in color and appear superimposed on the groundmass (Fig.27). It also fills intergranular space between quartz grains (Fig.28).

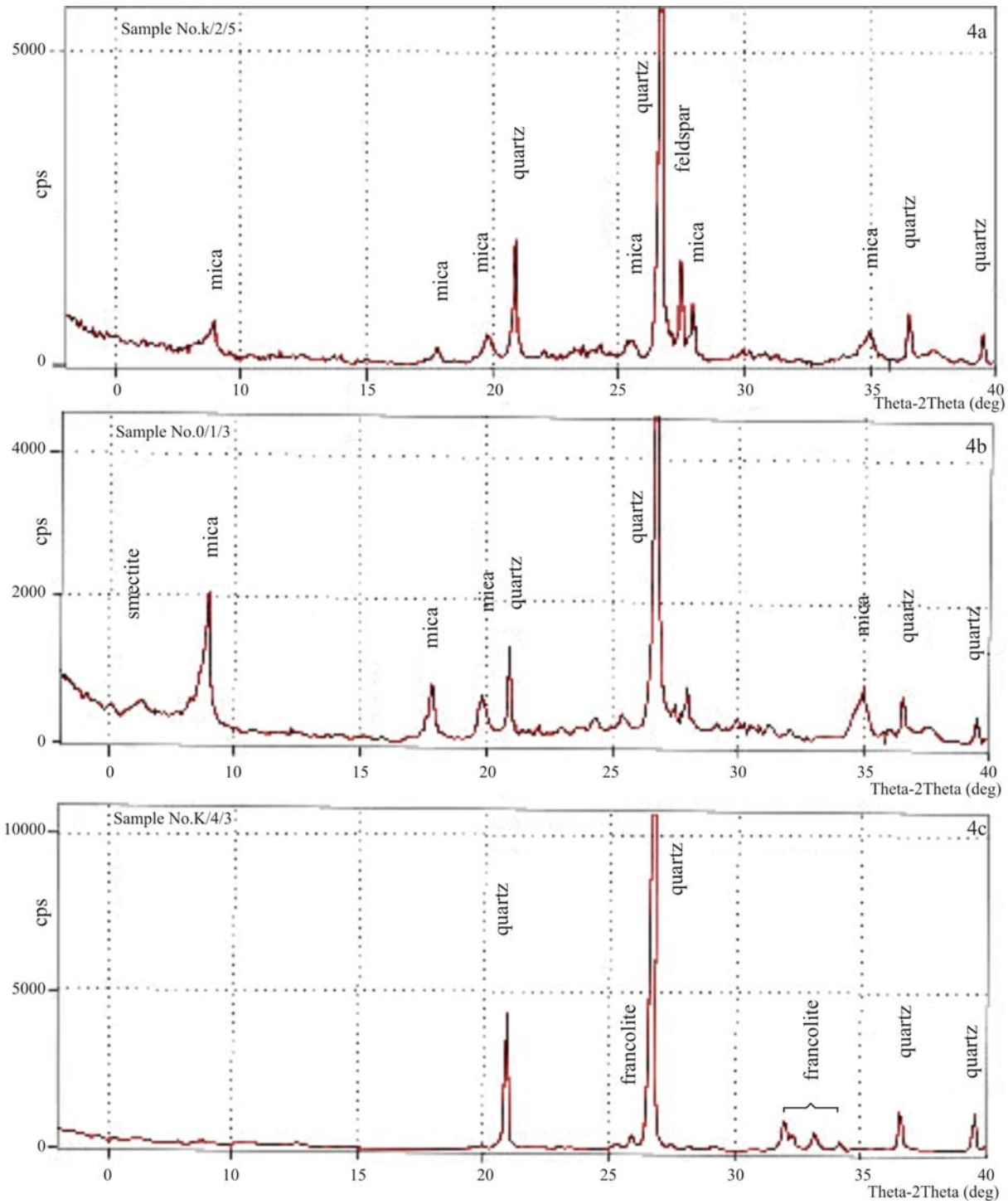

Fig.10: X-ray diffractograms of shale and sandstone samples (bulk samples)

a: Quartz arenite

b: Phyllarenite

c: Phosphatic quartz arenite

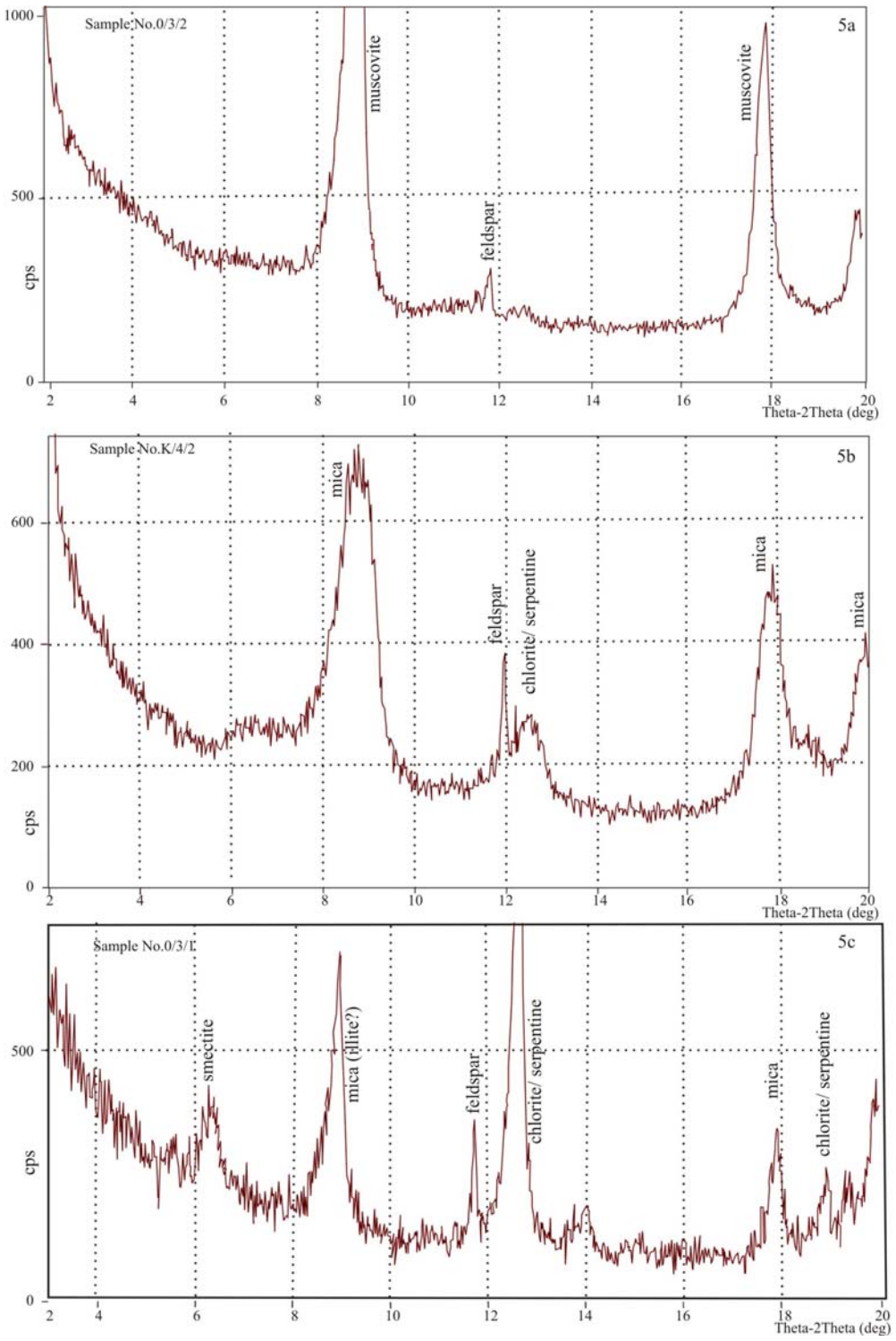

Fig.11: X-ray diffractograms of clay fraction separated from shale and sandstone samples
a: Shale, showing well-crystalline muscovite and traces of feldspar
b: Shale, showing several peaks at about 10Å indicating presence of more than one mineral of the mica group. It also shows minor presence of chlorite/serpentine.
c: Phyllarenite, showing major presence of chlorite/serpentine and single peak of mica (probably illite) and a rare presence of smectite. Feldspar is present, as minor mineral, in all samples of the clay fraction.

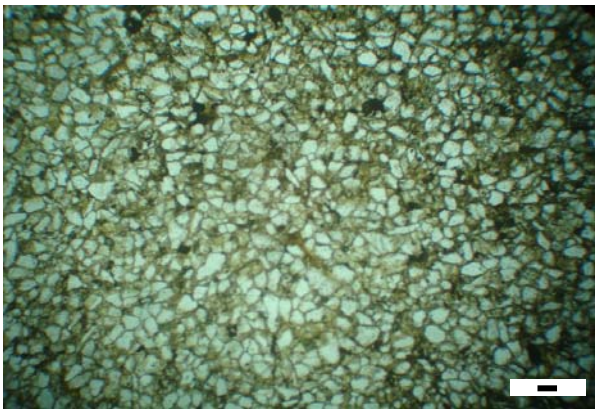

Fig.12, sample O/1/1

Fig.13, sample O/3/3

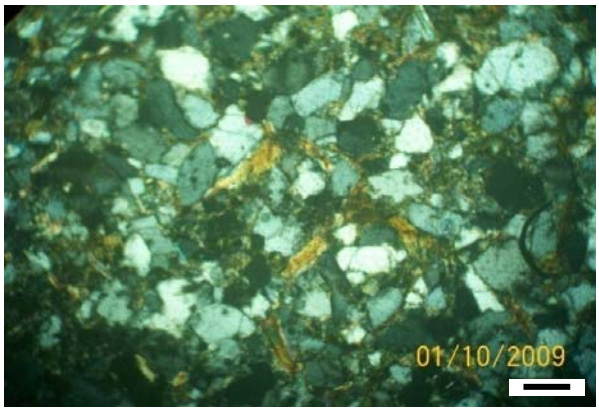

Fig.14, sample O/1/1

Fig.15, sample K/4/1

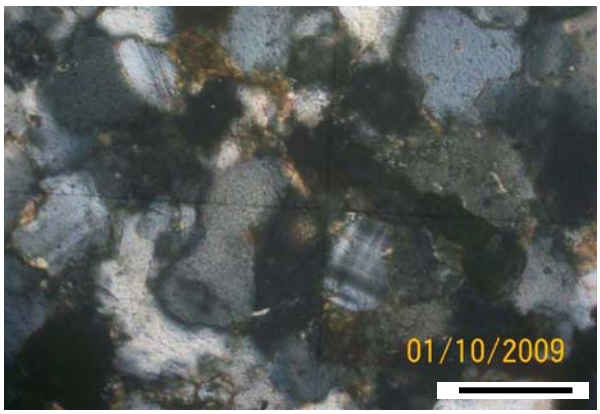

Fig.16, sample O/2/2

Fig.17, sample O/2/6

(Bar = 0.1 mm)
Fig.12: General texture of the Khabour Formation sandstone
Fig.13: Quartz arenite, showing interlocking crystals and “T” and “Y” junctions
Fig.14: Phyllarenite, showing micaceous matrix squeezed between quartz grains
Fig.15: Fresh plagioclase feldspar showing albite twining
Fig.16: Fresh microcline feldspar
Fig.17: Plagioclase feldspar showing diagenetic alteration to sheet silicates

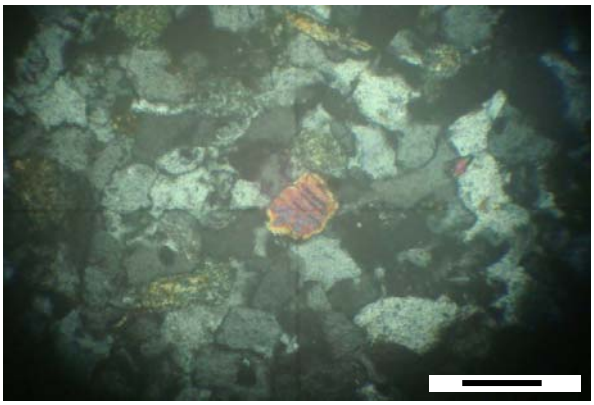

Fig.18a, sample K/3/1

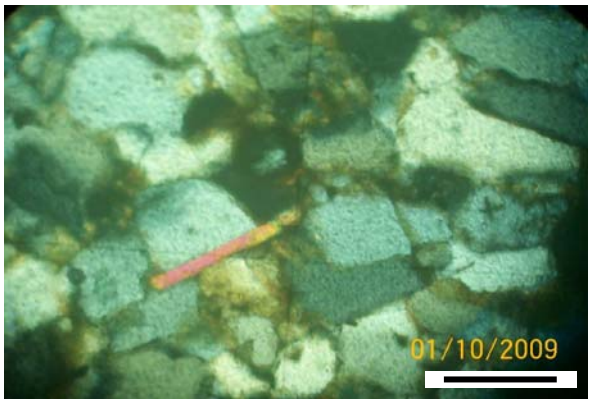

Fig.18b, sample O/3/3

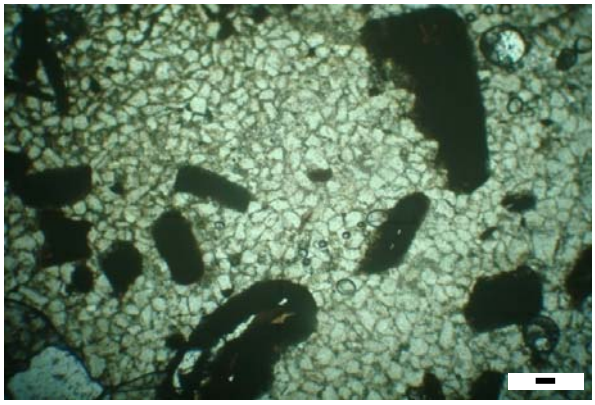

Fig.19, sample K/4/3

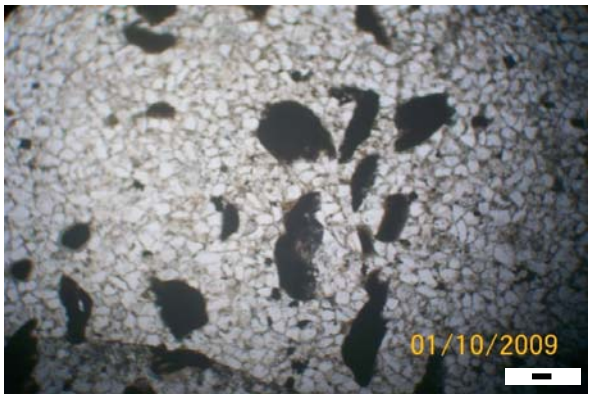

Fig.20, sample K/4/3

Fig.21, sample K/4/3

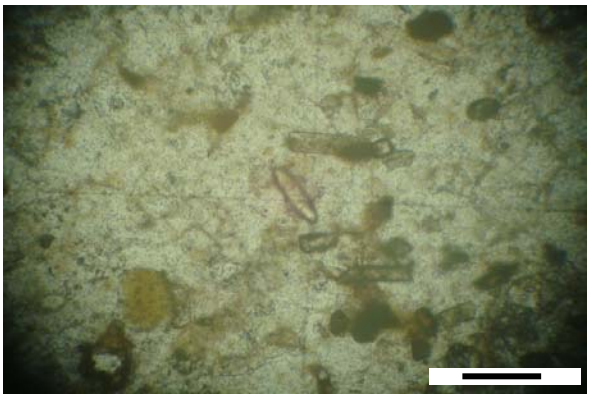

Fig.22, sample K/3/1

(Bar = 0.1 mm)
Fig.18a: Abraded detrital muscovite showing cleavage
Fig.18b: Authigenic mica
Fig.19: Conodont (?) skeletal remains composed of francolite, in quartz arenite
Fig.20: Phosphate (francolite) bioclasts in quartz arenite
Fig.21: Phosphate (francolite) cortoid in quartz arenite
Fig.22: Rounded zircon and elongated tourmaline (grains with high relief) in quartz arenite

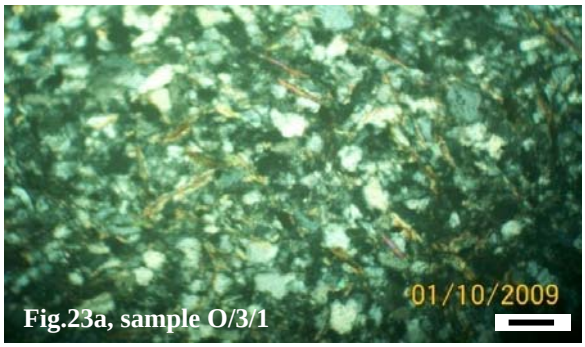

Fig.23a, sample O/3/1

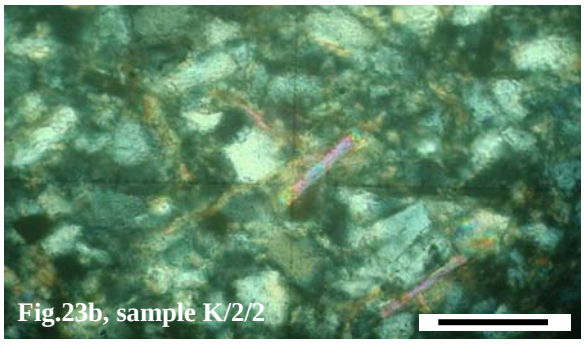
Fig.23b, sample K/2/2

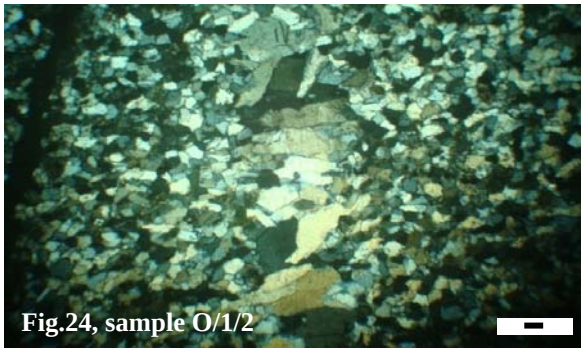
Fig.24, sample O/1/2

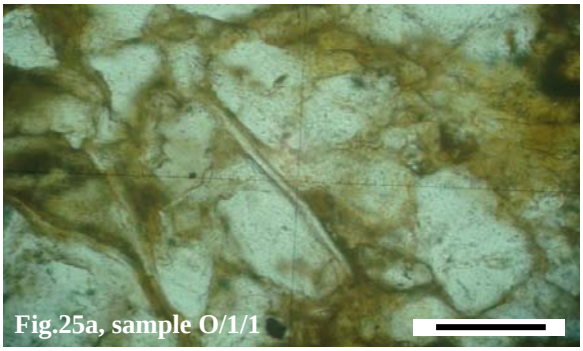
Fig.25a, sample O/1/1

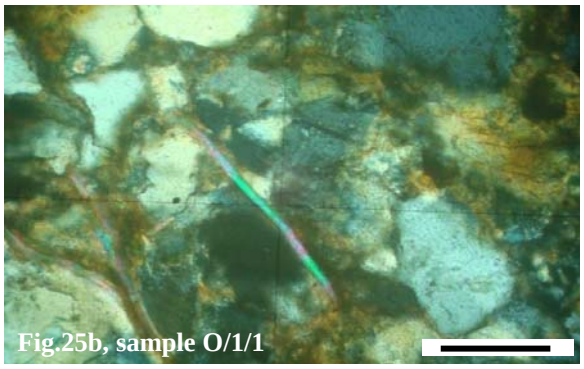
Fig.25b, sample O/1/1


Fig.26, sample O/3/4

Fig.27, sample K/1/1

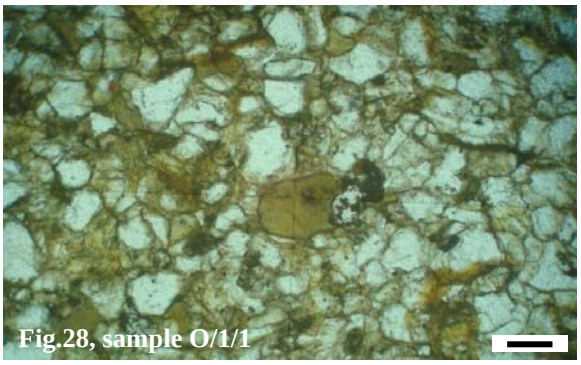
Fig.28, sample O/1/1

(Bar = 0.1mm)
Fig.23a: Phyllarenite with abundant mixed-layer chlorite/serpentine (elongated fibers)
Fig.23b: An enlargement of chlorite/serpentine fibers
Fig.24: Coarse crystalline quartz cement, filling fracture in quartz arenite
Fig 25a: Authigenic interstratified chlorite/serpentine coating quartz grains in phyllarenite
Fig.25b: Same as above under XN
Fig.26: Diagenetic chlorite/serpentine mixed layer filling stylolite space
Fig.27: Diagenetic glauconite grain in quartz arenite
Fig.28: Diagenetic glauconite matrix in phyllarenite

Table 1: Heavy mineral analysis

Sample No.	Wt. (gm) of (63 – 250) µm fraction	Weight %*		Number %									
		H.F	L.F	Opaques	Zircon	Tourmaline	Rutile	Chlorite	Zoisite – Epidote	Hornblende	Pyroxene	Alterites	Others
O/1/1	19.46	8.73	91.27	67.22	10.0	11.66	3.33	4.44	1.11	0.55	–	1.66	Staurolite T., kyanite T., garnet 1.11, barite and cellestite 0.55, biotite T.
O/1/2	22.63	7.25	92.75	74.76	11.21	7.94	2.80	T	0.47	–	0.93	1.87	–
O/2/2	15.12	7.27	92.73	62.11	7.05	7.93	2.64	6.17	3.08	1.76	3.08	2.20	Garnet 1.76, barite and cellestite 1.32, anatase 0.88
O/2/3	16.17	10.82	89.18	42.22	15.11	19.55	3.55	8.44	1.33	1.33	2.22	1.77	Garnet 1.33, barite and cellestite 0.44, anatase 1.33, titanite 1.33
O/3/4	17.37	8.63	91.37	40.26	9.73	11.50	2.21	30.92	1.77	0.88	–	0.88	Garnet 0.44, barite and celestite 0.88, anatase T., kyanite 0.44
K/2/2	23.19	10.86	89.14	27.60	32.81	30.21	8.07	0.53	0.26	–	–	–	Garnet T., titanite T., anatase 0.53
K/2/3	13.14	12.48	87.52	45.09	10.71	12.05	1.79	15.63	1.34	2.68	5.8	0.89	Staurolite T., anatase T., barite and cellestite 4.02, biotite T.
K/3/3	12.29	19.06	80.94	51.92	9.20	20.86	5.52	3.68	0.61	1.23	3.07	2.45	Barite and cellestite 0.61, anatase 1.23, kyanite 0.61

Table 2: Chemical composition (in wt.% except ZrO_2 in ppm)

Sample No.	SiO_2	TiO_2	Fe_2O_3	Al_2O_3	CaO	MgO	K_2O	Na_2O	P_2O_5	ZrO_2	L.O.I.
K/1/1	94.23	0.55	0.54	2.65	0.27	0.12	0.78	0.23	0.16	327	0.66
K/2/1	54.44	1.3	6.28	23.31	0.47	2.54	5.52	0.72	0.16	190	5.83
K/2/2	86.85	2.12	2.31	4.92	0.8	0.6	0.76	0.6	0.46	1382	1.12
K/2/3	75.07	1.0	3.55	12.44	0.84	1.37	2.26	2.0	0.15	346	2.54
K/2/4	81.13	0.97	3.38	9.33	0.51	1.02	1.09	1.98	0.14	525	1.78
K/2/5	64.67	0.94	5.69	17.62	0.44	1.28	4.87	1.08	0.14	439	4.04
K/3/1	86.93	0.4	3.59	4.82	0.12	0.33	1.83	1.06	0.1	427	1.49
K/3/2	82.34	0.7	2.9	8.88	0.19	0.61	2.97	0.43	0.13	210	1.06
K/3/3	67.88	1.22	5.42	15.37	0.37	1.27	4.63	0.78	0.15	392	3.63
K/4/1	86.43	0.61	3.26	5.67	0.25	0.38	1.46	0.37	0.19	317	1.73
K/4/2	79.04	0.82	5.25	8.76	0.45	0.69	1.96	0.31	0.28	276	2.74
K/4/3*	71.99	0.68	3.93	4.42	9.74	0.65	0.79	0.24	5.25	353	2.44
O/3/1	73.97	0.93	3.85	12.25	0.32	1.45	2.47	1.55	0.06	388	2.22
O/3/2	58.29	1.63	4.65	21.5	0.46	1.55	5.57	0.91	0.06	390	4.84
O/3/3	91.6	0.5	2.29	3.72	0.07	0.42	0.39	0.48	0.05	205	0.94
O/3/4	93.64	0.43	1.6	2.73	0.07	0.41	0.26	0.17	0.05	197	0.80
O/2/1	91.69	0.21	1.5	3.99	0.27	0.25	1.28	0.35	0.06	146	0.72
O/2/2	84.13	0.48	2.7	7.89	0.19	0.51	2.44	0.88	0.06	219	1.46
O/2/3	86.65	0.51	2.55	6.68	0.28	0.68	1.31	0.90	0.06	284	1.24
O/2/4	82.76	0.78	5.34	6.25	0.19	0.44	1.79	0.42	0.05	285	2.36
O/2/5	76.26	1.1	4.87	11.0	0.21	0.85	3.20	0.99	0.05	269	2.44
O/2/6	92.13	0.69	1.5	3.12	0.66	0.24	0.62	0.19	0.07	381	0.93
O/1/1	78.17	1.0	4.03	10.36	0.55	0.96	2.14	0.64	0.06	286	2.69
O/1/2	75.14	1.19	5.9	10.96	0.52	0.67	2.39	0.30	0.06	500	3.13
O/1/3	57.08	1.47	5.38	23.0	0.40	1.56	5.89	0.90	0.06	291	5.13
O/1/4	77.05	0.95	4.64	10.61	0.26	0.84	2.56	0.58	0.06	470	2.98

* Contains 0.5% F

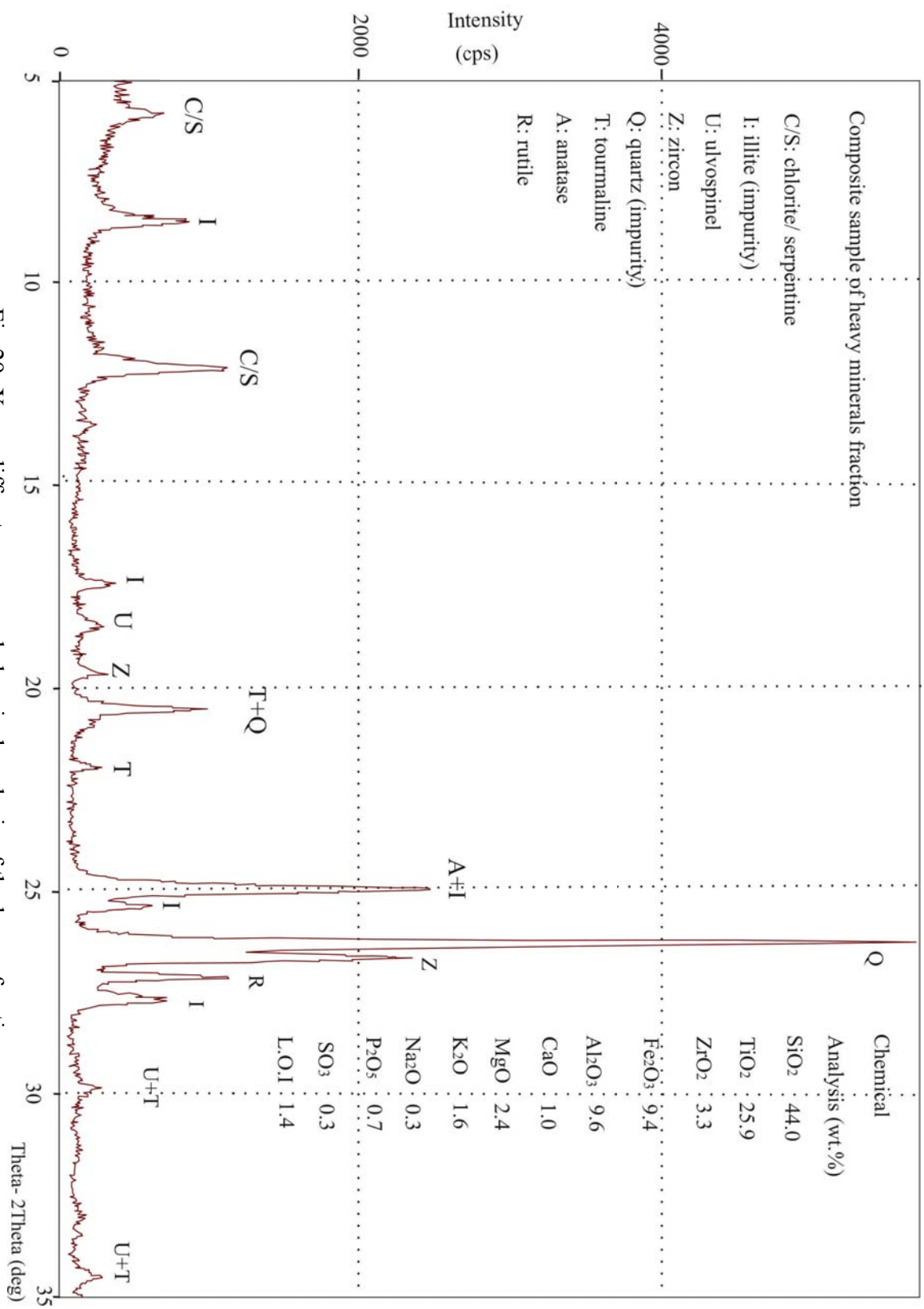

Fig.29: X-ray diffractograms and chemical analysis of the heavy fraction
(The sample contains impurities of quartz and mica)

CHEMICAL COMPOSITION AND GEOCHEMISTRY

The results of chemical analysis are presented in Table (2). The samples were separated into three groups according to their chemical, mineralogical and textural criteria, and the mean chemical composition was derived for each group (Table 3). Group 1 represents quartz arenite (more than 90% SiO_2), Group 2 represents phyllarenite (sandstones with less than 90% SiO_2) and Group 3 represents the shale.

The chemical composition is directly related to mineral composition and controlled by the relative proportions of quartz, muscovite-illite, glauconite and occasionally chlorite/serpentine. Francolite (in one sample) show some influence on chemical composition as well as the minor amounts of the heavy minerals (zircon, tourmaline, ulvospinel, anatase and rutile).

Silica is shared with almost all minerals; alumina is mainly related to sheet silicates (mainly muscovite-illite), feldspar and some heavy minerals like tourmaline. Potassium is mainly hosted by muscovite-illite and glauconite, iron oxide is mainly hosted by ulvospinel, tourmaline, illite, glauconite and chlorite (with some possible free Fe oxyhydroxide cement) whereas magnesia is related to chlorite/serpentine. Calcium, phosphorus and fluoride are strictly restricted to francolite. Titanium is related to rutile, ulvospinel and anatase, whereas zirconium is related to zircon. Some titanium, however, may be incorporated in the sheet silicates. Sodium may be related to tourmaline and feldspar.

The Khabour Formation consists of various proportions of these minerals; dominated by quartz in the quartz arenite with minor amounts of sheet silicate minerals and feldspar. SiO_2 content in this rock type is more than 90% and is characterized by a low Al_2O_3, K_2O, MgO and generally less than 1% H_2O^+ (L.O.I). The SiO_2/Al_2O_3 ratio is 28.6 and the K_2O/Na_2O ratio is 2.4. The quartz content decreases to a mean of about 50% in the phyllarenite with increasing proportions of the sheet silicates especially muscovite-illite (about 35%) and to a lesser extent (<10%) glauconite and minor chlorite, leading to higher concentrations of Al_2O_3, Fe_2O_3, K_2O and MgO related to these minerals, accompanied by a consequent increase of H_2O^+ (L.O.I) content to about 2%. The SiO_2/Al_2O_3 ratio decreases here to 9.3, whereas the K_2O/ Na_2O ratio is 2.2, which is close to that of the quartz arenite.

Shale samples consist of similar mineral assemblage, but with quartz (silt-size) content decreasing to about 25% and mica – illite content increasing to about 60%. Glauconite represents about 10% of the mineral composition of these shales.

This change in mineral proportions is reflected in lower SiO_2 and higher Al_2O_3, K_2O, MgO and Fe_2O_3. The L.O.I. $(H_2O)^+$ content increases to about 4% (mean value), released from hydrous sheet silicates. The SiO_2/Al_2O_3 ratio in these samples is 4.0 and the K_2O/Na_2O ratio is 5.9. Potter (1978) related high SiO_2/Al_2O_3 and high K_2O/Na_2O ratios to Atlantic-type passive margin big-river sands and distinguished them from collision-type coasts that have lowered such ratios.

Statistical analysis of the analytical data is in agreement with geochemical association of elements to the minerals identified in these samples (Table 4). Quartz, being almost free of ionic substitution and a major constituent of these rocks dominating the silica content, shows (as SiO_2) strong negative correlation with diluent's sheet silicate mineral constituents (such as Fe, Al, Mg, K and L. O. I). It shows insignificant correlation with Zr, P and Ca.

On the other hand, alumina, the representative oxide of the sheet silicate minerals and feldspars, is positively correlated with Fe, Mg, K and L.O.I. Titanium correlation is shared positively between the sheet-silicate constituents, as a substituent ion in the octahedral layer, evidenced by the positive correlation with Al, Mg, K and L.O.I. and with Zr as a member of the stable heavy mineral assemblage.

Table 4: Correlations coefficients

	SiO_2	Fe_2O_3	Al_2O_3	TiO_2	CaO	MgO	L.O.I	Na_2O	K_2O	P_2O_5
Fe_2O_3	-0.822									
Al_2O_3	-0.948	0.746								
TiO_2	-0.613	0.481	0.608							
CaO	-0.155	0.043	-0.144	-0.032						
MgO	-0.894	0.666	0.914	0.582	-0.029					
L.O.I	-0.965	0.856	0.937	0.593	0.044	0.861				
Na_2O	-0.329	0.204	0.398	0.226	-0.165	0.498	0.221			
K_2O	-0.900	0.728	0.954	0.518	-0.176	0.796	0.889	0.269		
P_2O_5	-0.119	0.022	-0.182	-0.058	0.995	-0.067	0.009	-0.202	-0.201	
ZrO_2	0.036	-0.034	-0.076	0.658	0.049	-0.036	-0.069	0.116	-0.138	0.054

Table 3: Mean chemical composition of main rock types (in wt%)

	Quartz arenite	Phyllarenite*	Shale
SiO_2	92.66	80.15	66.31
TiO_2	0.48	0.90	1.17
Fe_2O_3	1.49	3.68	5.43
Al_2O_3	3.24	8.59	16.54
CaO	0.27	0.39	0.40
MgO	0.29	0.78	1.33
K_2O	0.67	1.98	4.32
Na_2O	0.28	0.89	0.73
P_2O_5	0.08	0.12	0.19
ZrO_2 (ppm)	251	427	323
LOI	0.81	2.02	4.08
Number of samples	5	13	7

*Mean, excluding sample K/4/3 (phosphate-bearing)

Quartz arenite: Samples K/1/1, O/3/4, O/2/1, O/2/6 and O/3/3
Phyllarenite: Samples K/2/2, K/2/3, K/2/4, K/3/1, K/3/2, K/4/1, K/4/3, O/3/1, O/1/4, O/2/2, O/2/3, O/2/5, O/1/1 and O/1/2
Silty shale: Samples K/2/1, K/2/5, K/3/3, K/4/2, O/3/2, O/2/4 and O/1/3

The TiO_2 content of the heavy fraction is shared between rutile, ulvospinel and anatase. Together they make about one third of the heavy fraction constituents. The chemical analysis of a composite sample of heavy fractions, separated by bromoform from sandstone samples of Table (1), showed about 26% TiO_2 and 3% ZrO_2. These results suggest that the Khabour Formation may be looked at as a potential Ti and Zr resource and deserves further investigation.

Francolite emphasizes its presence by strong positive correlation between P_2O_5 and CaO approaching almost unity (Table 4). Sodium has no decisive correlation with any of the elements analyzed. It shows weak, but significant positive correlation with Mg and Al. It is shared between the feldspars and sheet silicates.

Factor analysis revealed three major factors that explain about 86% of variance (Table 5). Factor 1, explains about 53% of variance and positively dominates the behavior of the chemical constituents of the sheet silicate minerals (Al, Fe, Mg and K) and has negative correlation with the silica. This factor may be related to energy of the depositional environment. A quiet environment permits settling of these micaceous minerals whereas agitated and stormy environment, where the quartz arenite was deposited, hinder any settlement of these minerals. This factor may be an indicator of depth and energy also.

Factor 2, explains about 19% of variance, and is controlling phosphate formation and precipitation of francolite in these sandstones. In view of the limited occurrence of francolite in the studied samples and authigenic nature (cortoids) or detrital nature (scales and intraclasts), this factor may be related to limited episode of phosphogenesis that can be related to the onset of a transgressive cycle with P-rich deeper waters welling up to shallow parts of the basin in one of the multiple (MFS) events accompanied the (AP_2) megacycle.

Factor 3 controls Zr and Ti and explains about 14% of variance. Both elements are mainly found in the heavy minerals (zircon, rutile, anatase and ulvospinel) and the factor may express maturity of the detrital components as well as provenance.

Table 5: Factor analysis

	Component		
	1	**2**	**3**
SiO_2	-0.972	-0.209	0.082
Fe_2O_3	0.831	0.131	-0.110
Al_2O_3	0.980	-0.097	-0.088
TiO_2	0.677	0.050	0.674
CaO	-0.059	0.986	-0.029
MgO	0.923	-0.003	-0.029
L.O.I	0.961	0.119	-0.123
Na_2O	0.408	-0.259	0.198
K_2O	0.924	-0.119	-0.176
P_2O_5	-0.095	0.986	-0.031
ZrO_2	0.025	0.096	0.977
% of variance	53.3	19.3	13.8

Significant value = 0.4

DISCUSSION

▪ Source Rocks

The petrology of the studied samples suggests two types of source rocks; a granitic plutonic rocks, reworked and recycled several times, suggested by the fine grained, well-sorted quartz arenite, monocrystalline quartz and dominant (ZTR) minerals in the heavy fraction. The apparent angularity of the quartz grains is caused by late digenetic interlock of more rounded quartz grains and cementation by silica under burial compaction causing pressure solution. First cycle sands are apt to be less rounded and to contain a greater proportion of polycrystalline and undulatory quartz and contain a great diversity of heavy minerals (Folk, 1974).

A second source of the clastics and more proximal one appears to have been a low-grade metamorphic rock, rich in micaceous minerals such as slates, phyllites and green schists. The clasts of these rocks seem to have suffered less reworking in view of the fresh appearance of

the micaceous minerals and their larger size compared to quartz. Because of the softness of the slate and phyllite fragments, they are abraded away producing great volumes of clay-mica mush which are winnowed out of the sands to produce thick shale horizons (Folk, 1974). This is supported by the presence of mixed-layer chlorite/serpentine and some diagnostic heavy minerals (Table 1).

- **Maturity**

Textural maturity is represented by the relative abundance of matrix and degree of rounding and sorting of framework grains (Boggs, 2006). In this sense, the basal parts of the sedimentary cycles of the Khabour Formation may be considered mature to supermature, grading upward to submature with the introduction of the micaceous matrix.

On the other hand, compositional (mineralogical) maturity is estimated by the relative abundance of stable and unstable grains (Boggs, 2006) and may be represented by the ratio of quartz (stable) to feldspar or rock fragments (unstable or less stable). Mica (as muscovite) is considered as a mechanically stable mineral and, under cold climate and/ or arid conditions, a chemically stable mineral (Krumbein and Sloss, 1963). In this sense the studied sandstones can be considered fairly mature.

- **Paleogeography and Paleoclimate**

The low rate of alteration found in the feldspar and mica suggests cool and/ or arid climate. Iraq and the rest of Arabia were located at about 40° latitude south of the equator during the Ordovician time (Beydon, 1993). The Saharan glaciation's affected the western parts of the Arabia, which was at that time at its lowest southerly latitude (Sharland *et al*., 2001, Jassim and Goff, 2006). This palaeogeographic position induced cool climate and lower sea-level. The cool climate is supported by the fresh feldspar grains (Figs.15 and 16) and their persistent presence in the fine fraction (Fig.11).

- **Depositional Environment**

The Khabour Formation in the studied sections comprises a sequence of graded beddings of quartz sand, silt and micaceous shale. All of which appear to have been deposited in marine environment ranging from intertidal to outer shelf realms. The marine fauna and *Cruziana* trails as well as the common presence of glauconite and occasional francolite (with conodont remains) are evidence of the marine environment.

Wetzel (1950) suggested deposition in a tide-and storm-dominated shallow marine intertidal environment of mud-and silt-flats. The results of the present study can not verify storm-dominated mud or silt-flat environment for these clastics. The storm-dominated shelf deposits are usually quite complex and show thin layers consisting of concentrations of coarser grains interlayered or embedded in finer-grained mud (Krumbein and Sloss, 1963 and Boggs, 2006). Moreover, tidal flat deposits are usually rich in marine life and highly oxygenated, because of intermittent exposure. Seilacher (1963), on the other hand, suggested turbidite facies for the upper part of the sequence, which seems an acceptable model.

Graded bedding may form by sedimentation from suspension clouds or last phases of heavy floods, but most of these graded beds of marine origin in the geologic record have been attributed to turbidity currents (Boggs, 2006). Most turbidities are composed of sands, silty sands (or gravelly sands) interbedded with pelagic clays. They are commonly characterized by normal-size grading and may or may not display complete Bouma sequence (Boggs, 2006). In the present study a complete Bouma sequence was not observed. A stack of complete Bouma sequences overlying each other in a cyclic manner assumes no change in sea-level and the only variable is the successive episodes of density currents supplying clastics to the marine

environment, and the sediment supply should be almost equal to subsidence rate, allowing for a constant accommodation space. Such ideal conditions were never the case, as these variables acted indifferently. This may partly explains the absence of a complete and ideal Bouma sequences stacked in a cyclic manner in the studied sections.

In the opinion of the author, most of the cyclic succession of the Khabour Formation may be assigned to deposition from turbidity currents of submarine fan environment under variable sea-level, subsidence rate and sediment supply. The quartz arenites (basal deposits of the cycles) represent the proximal parts of the fan, deposited in intertidal, very shallow agitated environment, gradually passing into deeper subtidal outer shelf facies with a high appearance of micaceous minerals and *Cruziana* trails, which represent the distal part of the fan. The occasional presence of wave ripples (observed by previous workers) in the lower part of the sequence where medium-and fine grained sandstones dominates the sequence, indicates high density turbidity currents and suggests that the seabed was often within storm waver-base (50 – 100) m. (Rieu and Allen, 2008). Their presence indicates shallow turbidite system fed by rivers rather than a deep-sea turbidite (Plink-BjOrklund and Steel, 2004). On the other hand, the laminated greenish shale and siltstone in the upper part of the sequence with slump structures associated with thin graded sandstones indicates a quiet, distal-marine depositional environment dominated by deep outer shelf hemi pelagic sedimentation. It represents outer fan facies association and low density turbidity currents (Rieu and Allen, 2008). The whole sequence may be considered as an example of a passive plate margin turbidities influenced by variable sea-level and sediment supply. The relatively high SiO_2/Al_2O_3 and K_2O/Na_2O ratios are related to Atlantic-type passive margin sand deposits (Potter, 1978). Pettijohn *et al.* (1986) stated that submarine fans on the continental shelf bellow submarine canyons show greater abundance of micas farther out on the fan, whereas the more proximal parts of the fan are coarser grained and contain less mica.

The cyclicity of the sequence might have been partly induced by episodes of floods supplying clastics from source rocks exposed at higher altitudes of the Afro-Arabian craton and transported to the marine realm via turbidity currents, or by pulses of sea-level fluctuations. Sea-level fluctuations may be related to tectonic pulses leading to higher subsidence rate, or eustatic periodical changes related to glaciation's intensity at the poles.

During the Middle and Late Ordovician, a gradual rise in sea level resulted in the development of an intracratonic marine shelf basin (Jassim and Goff, 2006). The sudden increase in subsidence was attributed by Oterdoom *et al.* (1999) to rifting across Arabia, and thought to have brought the outer-shelf shales to be rapidly deposited above inner-shelf and continental coarse clastics. The relatively deeper shelf conditions were suddenly terminated by a drop of sea level triggered by the Saharan glaciations, which resulted in highly incised land forms and submarine canyons in NW Arabia (Husseini, 1991 and 1992).

Sharland *et al.* (2001) mentioned that the lithological changes during (AP2), from relatively undifferentiated coarse clastics to alternating shale-sand associations suggests significant changes in relative sea-level, accommodation space and sediment supply. AP2 (520 – 445 M.a.) was deposited during passive subsidence (Jassim and Goff, 2006). Within AP2, several MFS's were recognized, represented by the shale beds in the sequence, and indicate transgressive phases. The 040 MFS is Late Ordovician (Late Caradoc) dated as 453 M.a. and is correlatable with the shale in the middle of the Khabour Formation (Aqrawi, 1998).

These successive transgressive – regressive episodes seem to have been more frequent and short-lived in the early stages, followed by longer transgressive stands in the later stages, allowing for thicker distal outer shelf shale sediments to dominate the middle and upper parts of the sequence. The partings (surfaces) between one cycle and the next represents a second

order (MFS) where deposition may stand still or becomes very slow evidenced by burrowed and pitted surfaces and common presence of glauconite and occasional francolite; both are indicators of condensed sections of non-or slow-deposition (Pettijohn *et al*., 1986). The non- or slow-deposition may have been caused by decreasing influence of the turbidity currents which retreated shore-ward due to high sea-level stand and consequent retreat of the feeding source further insides the continent.

Successive density currents, passing over previous deposits may lay down additional graded bed without seriously disturbing the relatively fine upper surface of previous cycle, although surface markings may occur (Krumbein and Sloss, 1963). Many of these surface markings were noticed by previous authors in the studied sequence (Wetzel, 1950, Al-Hadithi, 1972 and Isaac, 1975).

The erosional unconformity, marking the uppermost part of the Khabour Formation, may have removed significant sedimentary record of the retreating glaciation of the Ashgill (Jassim and Goff, 2006). The missing upper part of the formation was encountered in many subsurface sections.

- **Digenesis**

Early diagenetic processes include partial and minor alteration of feldspars, illite transformation to chlorite, and formation of digenetic muscovite and deposition of glauconite. Deep burial of the Khabour Formation clastics caused some later diagenetic alterations, mainly pressure-solution and reprecipitation of silica, probably some smectite transformation to illite, partial removal of Fe from chlorite, development of chlorite/ serpentine mixed layer and the break down and squeeze of the detrital mica flakes between the much harder quartz grains, by compaction pressure, forming the matrix material in the matrix-bearing arenites. No sign of metamorphic alterations were noticed, except those related to deep burial.

CONCLUSIONS

- The clastics of the Khabour Formation were derived from two probable sources: a recycled granitic plutonic rock and more proximal low-grade (phyllitic) metamorphic rocks.
- The sandstones are texturally mature to supermature and mineralogically fairly mature. The sandstones are of two types: quartz arenite (more than 90% interlocking quartz grains) and phyllarenite (mostly quartz and mica). The shale consists of silt-size quartz and micaceous minerals. Feldspar is a minor to trace constituent.
- Glauconite and francolite are the main authigenic minerals. The latter may be related to conodonts, and marks the earliest marine phosphate showing in Iraq. A mixed-layer chlorite/ serpentine is an alteration product and marks deep burial. Silica cementation is the main diagenetic process induced by pressure solution due to burial.
- The whole sequence is marine in origin, deposited in environments ranging from agitated intertidal to calm deep outer shelf environments.
- The cyclicity of the sequence may be explained as due to several factors including sea-level fluctuations (tectonic and eustatic) and supply rate of detritus to the depositional environment. However, the cyclicity may be interpreted by successive density currents and the whole sequence may be considered as an example of a passive extensional plate margin turbidities.

ACKNOWLEDGMENTS

The author is indebted to Dr. Saffa A. Fouad, Mr. Varoujan K. Sissakian and Mr. Sabah Y. Yacoub (GEOSURV Experts) for their valuable help in locating the studied sections and help during fieldwork. The stimulating discussions with Professor Mazin Tamar-Agha and

Dr. Saffa Fouad enlightened the author on many aspects related to the concept of this paper. Their comments on the manuscript were valuable and highly appreciated. The heavy minerals were identified and counted by Mrs. Luma E. Al-Mukhtar (GEOSURV Central Laboratories). The hard work by Miss. Mariamme A. Kaka and Miss. Zainab S. Haddu in typing, editing and computer cartography is highly appreciated.

REFERENCES

Al-Hadithi, T.M., 1972 (revised by Pesel, V., 1974). Geological stage report on Sereru area, Northern Iraq. GEOSURV, int. rep. no. 655.

Al-Janabi, Y., Al-Sa'adi, N., Zainal, Y., Al-Bassam, K., and Al-Delaimy, M., 1992. GEOSURV Work Procedures, Part 21: Chemical Laboratories. GEOSURV, int. rep. no. 1991.

Aqrawi, A.A.M., 1998. Paleozoic stratigraphy and petroleum systems of the Western and Southwestern Deserts of Iraq. GeoArabia, Vol.3, p. 229 – 248.

Beydoun, Z.R., 1991. Arabian Plate hydrocarbon geology and potential: A plate tectonic approach. Studies in Geology, AAPG, Vol.33, 77pp.

Boggs, S. Jr., 2006. Principles of Sedimentology and Stratigraphy, 4th edit. Pearson/ Prentice Hall, New Jersey, 662pp.

Buday, T., 1980. The Regional Geology of Iraq. Vol.1, Stratigraphy and Paleogeography. In: I.I. Kassab and S.Z. Jassim (Eds.). GEOSURV, Iraq, 445pp.

Cooper, B.J., 1981. Early Ordovician conodont from the Horn Valley siltstone, Central Australia. Paleontology, Vol.24, p. 147 – 183.

Ditmar, V. and Iraqi – Soviet Team, 1971. Geological conditions and hydrocarbon prospects of the Republic of Iraq (Northern and Central parts). Ministry of Oil (INOC), internal report.

Folk, R.L., 1974. Petrology of Sedimentary Rocks. Hemphill Publishing Co., Austin Texas, 182pp.

Gaddo, J. and Parker, D., 1959. Final report on well Khleisia No.1. MPC int. rep. (Ministry of Oil, INOC Library, no. FWR 28).

Grigsby, J.D., 2001. Origin and growth mechanism of authigenic chlorite in sandstones of the Lower Vicksburg Formation, South Texas. Jour. Sedimentary Research, Vol.71, p. 27 – 36.

Habba, Y., Sammarai, A., Al-Jubouri, F., Georgis, N. and Ahmed, I., 1994. Exploration for the Paleozoic prospects in Western Iraq. Part 1: Exploration of the Paleozoic systems in Western Iraq. Proceedings of the 2nd Seminar on Hydrocarbon Potential of Deep Formations in the Arab Countries (OAPEC), Cairo (in Arabic).

Husseini, M.I., 1991. Tectonic and depositional model of the Arabian and adjoining plates during the Silurian – Devonian. AAPG, Vol.75, p. 108 – 120.

Husseini, M.I., 1992. Upper Paleozoic tectono-sedimentary evolution of the Arabian and adjoining plates. Jour. Geol. Soc., London, Vol.149, p. 419 – 429.

Isa'ac, E.A., 1975. Geology of the Dafaf – Keshan area, Northern Thrust Zone. GEOSURV, int. rep. no. 659.

Jassim, S.Z. and Goff, J.C. (Eds.), 2006. Geology of Iraq. Dolin, Prague and Moravian Museum, Brno, 340pp.

Krumbein, W.C. and Sloss, L.L., 1963. Stratigraphy and Sedimentation. W.H. Freeman and Co., London, 2nd edit., 660pp.

Muller, K.J., 1978. Conodont and other phosphatic microfossils. In: B.U., Hakand and A., Boersma (Eds.), Introduction to Marine Micropaleontology. Elsevier, New York, p. 277 – 291.

Oterdoom, W.H., Worthing, M.A. and Partington, M., 1999. Petrological and tectonostratigraphic evidence for a mid Ordovician rift pulse on the Arabian Peninsula. GeoArabia, Vol.4, p. 467 – 500.

Pettijohn, F.J., Potter, P.E. and Siever, R., 1986. Sand and Sandstone. Springer-Verlag, 2nd edit., 553pp.

Plink-BjOrklund, P. and Steel, R., 2004. Initiation of turbidity currents: Evidence for hyperpycnal flow turbidities in Eocene Central Basin of Spitsbergen. Sed. Geol., Vol.165, p. 29 – 52.

Potter, P.E., 1978. Petrology and chemistry of modern big river sands. Jour. Geology, Vol.86, p. 423 – 449.

Reynolds, R.C., Di Stefano, M.P. and Lahann, R.W., 1992. Randomly interstratified serpentine/chlorite; its detection and quantification by powder X-ray diffraction methods. Clays and Clay Minerals, Vol.40, p. 262 – 267.

Rieu, R. and Allen, P.A., 2008. Siliciclastic sedimentation in the interlude between two Neoproterozoic glaciation, Mirbat area, Southern Oman: A missing link in the Huqf Supergroup? GeoArabia, Vol.13, p. 45 – 72.

Seilacher, A., 1963. Kaledonischer Unterbau der Irakiden. Neuses Jahrb. Geol. Planet. Abt. Monatshefte, No.10, p. 527 – 542.

Sharland, P.R., Archer, R., Casey, D.M., Davies, R.B., Hall, S.H., Heward, A.P. Harbury, A.D. and Simmons, M.D., 2001. Arabian Plate Sequence Stratigraphy. GeoArabia, Special Publ., No.2, Gulf Petrolink, 371pp.

Tamar-Agha, M. and Mahdi, A., 1992. GEOSURV Work Procedures, Part 18: Petrology and Paleontology Laboratories. GEOSURV, int. rep. no. 1999.

Tamar-Agha, M., 2009. The influence of cementation on the reservoir quality of the Risha Sandstones Member (Upper Ordovician), Risha Gas Field, NE Jordan. Jour. Petroleum Geology, Vol.32, p. 193 – 208.

Wetzel, R., 1950. Khabour Quartzite Formation. In: Bellen, R.C., van, Dunnington, H.V., Wetzel, R. and Morton, D., 1959; Lexique Stratigraphique International. Asie, Fasc. 10a, Iraq. Paris, Vol.3, 333pp.